



An efficient one pot conversion of glycerol to lactic acid using bimetallic gold-platinum catalysts on a nanocrystalline CeO₂ support



Rajeesh Kumar Pazhavelikkakath Purushothaman ^{a,b}, J. van Haveren ^b,
D.S. van Es ^b, I. Melián-Cabrera ^a, J.D. Meeldijk ^c, H.J. Heeres ^{a,*}

^a Faculty of Mathematics and Natural Sciences, Department of Chemical Engineering, University of Groningen, Nijenborgh 4, 9747 AG Groningen, The Netherlands

^b Food and Bio-based Research, Department of Sustainable Chemistry, Wageningen University and Research Centre, Bornse Weilanden 9, 6700 AA Wageningen, The Netherlands

^c Electron Microscopy Department, Utrecht University, Padualaan 8, 3584 CH Utrecht, The Netherlands

ARTICLE INFO

Article history:

Received 16 April 2013

Received in revised form 26 July 2013

Accepted 30 July 2013

Available online 23 August 2013

Keywords:

Glycerol

Lactic acid

Gold

Bimetallic catalysts

Nanocrystalline ceria

ABSTRACT

The one pot conversion of glycerol to lactic acid using monometallic Au and Pt as well as bimetallic (Au–Pt) catalysts supported on nanocrystalline CeO₂ (*n*-CeO₂) in aqueous solution in the presence of a base and oxygen was investigated. Catalytic performance of the bimetallic catalysts is considerably better than the monometallic ones and is indicative for synergistic effects. The bimetallic system shows excellent activity (TOF = 1170 h⁻¹ for a batchtime of 20 min) with a high selectivity (80%) to lactic acid at 99% glycerol conversion (373 K, NaOH to glycerol ratio of 4 mol/mol 5 bar oxygen). The Au–Pt/*n*CeO₂ catalyst was recycled 5 times in a batch set-up without a significant drop in activity and lactic acid selectivity, indicative for good catalyst stability.

© 2013 Elsevier B.V. All rights reserved.

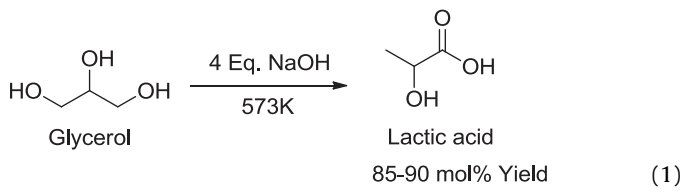
1. Introduction

The catalytic conversion of glycerol to green bulk chemicals is currently being researched actively [1–3]. One of the main drivers is the surplus of glycerol as a result of the growing biodiesel production levels in the period 1998–2010. Gold, previously being considered as an inert metal, shows very good catalytic activity when present as nano particles [4,5] and catalytic transformations using gold are now well established [6–10]. For instance, glycerol can be oxidised selectively to glyceric acid at aqueous alkaline conditions in a temperature range of 303–333 K [11–14] using gold nanoparticles on various supports. Interactions between the support and the gold nanoparticles are of paramount importance and determine the activity and selectivity of the oxidation reactions [15,16]. Catalyst performance can be improved significantly by the incorporation of a second metal such as palladium or platinum [17–22]. Best performance is obtained when both metals are present as nano-sized clusters in a single phase [23].

Lactic acid (2-hydroxy propionic acid) is an interesting bi-functional molecule. It is used as a monomer for the production of biodegradable polymers (polylactic acid) as well as for the

production of biodegradable, nontoxic solvents (lactic acid esters) [24,25]. It also has applications in the food, cosmetic, and pharmaceutical industry [24]. Lactic acid is considered a top 12 biobased platform molecule and may serve as a starting point for a wide range of future biobased chemicals by catalytic routes [26,27]. Lactic acid can be produced either chemically or biotechnologically by fermentation routes. The chemical route using HCN and acetaldehyde is of less interest nowadays due to environmental concerns. The current commercial process involves fermentation of various carbohydrates sources. However, both low space time yields and the difficult recovery of lactic acid from the fermentation broth have a major impact on the production costs [2] and alternative catalytic processes for the production of lactic acid are highly desirable.

Base catalysed conversions of glycerol to lactic acid at elevated temperatures have been reported. For instance, Kishida et al. showed that lactic acid can be obtained from glycerol by a hydrothermal treatment at 573 K in strong alkaline conditions up to a yield of 90 mol% after 1.5 h reaction time (Eq. (1)) [28]



* Corresponding author. Tel.: +31 50 363 4174; fax: +31 50 363 4479.

E-mail address: h.j.heeres@rug.nl (H.J. Heeres).

Higher glycerol concentrations were applied by Lopez et al., which resulted in 84% lactic acid yield in 1.5 h at 553 K [29]. KOH has superior activity compared to NaOH in the reaction [30]. The severe reaction conditions, viz. a high reaction temperature coupled with the necessity for a large amount of base, are a major concern for further scale up of this synthetic methodology.

Catalytic conversions of glycerol to lactic acid using heterogeneous catalysts have also been explored, both under reductive and oxidative conditions. Maris et al. observed lactic acid formation during the hydrogenolysis (473 K, 40 bar H₂) of glycerol in base solutions using monometallic (Ru and Pt) and bimetallic (PtRu and AuRu) on a carbon support. A lactic acid selectivity up to 62% (25% glycerol conversion) for Pt/C and 60% (21% conversion) for AuRu/C were obtained, though the selectivity decreased considerably at higher glycerol conversions [31,32]. ten Dam et al. also noticed lactic acid formation (55% selectivity at 46% glycerol conversion after 18 h) for the hydrogenolysis of glycerol using Pt/CaCO₃ in combination with boric acid (glycerol to boric acid ratio of 1, pH 12, 473 K, 40 bar H₂) [33]. Lactic acid formation under oxidative conditions have also been investigated. Shen et al. recently showed that monometallic Au and bimetallic Au–Pt on a TiO₂ support are selective catalysts for the conversion of glycerol to lactic acid at 363 K in strong alkaline conditions in an oxygen atmosphere [34]. A turn over frequency (TOF) of 520 h⁻¹ and a lactic acid selectivity up to 86% at 30% glycerol conversion was reported. Ir/CaCO₃ catalysts have also been reported for the conversion of glycerol to lactic acid in water. A lactic acid yield of 18% was obtained at 453 K after 6 h in the presence of 1 M NaOH in an inert atmosphere [35].

In this paper, we report the one pot conversion of glycerol to lactic acid in water under oxidative conditions using monometallic and bimetallic Au and Pt based catalysts on a nanoceria support. This support was selected as it is known that Au on nano-crystalline CeO₂ is an efficient oxidation catalyst for alcohols to aldehydes and ketones [36]. The high efficiency of nano-crystalline CeO₂ compared to regular (non-nanoparticulated) CeO₂ is supposed to be related to its ability to stabilise O₂ as superoxide and peroxide species [37]. Recently, Hutchings et al. showed the potential of bimetallic Au–Pd on nano-ceria for the oxidative esterification of 1,2 propanediol in methanol to methyl lactate up to a selectivity of 70–75% at 30–39% conversion [38].

However, catalysts based on the combination of nanoceria and noble metals like Au and Pt have not been explored for glycerol conversion in aqueous media in the presence of oxygen. In this study, the effect of the catalyst composition on lactic acid yields have been determined and relevant by-products have been identified. A reaction mechanism is proposed based on the experimentally observed activity and selectivity trends, supported by literature data.

2. Experimental

2.1. Materials

HAuCl₄·3H₂O (\geq 99.9%), K₂PtCl₆ (99.99%), Ceria (nano powder <25 nm, product code: 544841; 47 m²/g and 0.169 cm³/g), polyvinyl alcohol (PVA, M_w 13.000–23.000), NaBH₄ (\geq 98%) and NaOH (\geq 98%) were procured from Sigma–Aldrich. Activated carbon was obtained from Norit (SX1G, 854 m²/g and 0.642 cm³/g) and TiO₂ (P25, 50 m²/g and 0.352 cm³/g) was a gift from Evonik. Bulk CeO₂ was obtained from the Boreskov Institute for Catalysis, Russia (21 m²/g and 0.009 cm³/g). Oxygen (99.995%) was obtained from Linde Gas Benelux B.V., the Netherlands and hydrogen (9.86 vol% in nitrogen) from Praxair, Belgium.

2.2. Catalyst characterisation

Scanning Transmission Electron Microscope (STEM) images were recorded on Philips Tecnai F20 FEG electron microscope fitted with an X-ray EDS system operating at 200 kV. The images were acquired with Fischione High Angle Annular Dark Field (HAADF) detector. Catalyst samples were finely powdered and dispersed in ethanol. A small droplet of this dispersion was deposited on a copper grid coated with carbon. Particle size distributions of the catalysts were determined from the transmission electron micrographs by measuring the dimensions of a number of particles.

Aberration-corrected high-resolution STEM images were acquired using a XFEG FEI TITAN 60–300 kV equipped with an EDS detector (EDAX), a monochromator and a spherical aberration corrector for the electron probe (CEOS). The microscope was operated at 300 kV achieving a 0.08 nm resolution.

Pore volumes and BET surface areas were experimentally determined by N₂ physisorption at –196 °C using an ASAP 2420 instrument.

X-ray photoelectron spectroscopy (XPS) was used to study the chemical composition and the oxidation state of the elements on the catalyst surface. The XPS instrument, a VG Escalab 200 R spectrometer with a MgK α X-ray source ($h\nu$ = 1253.6 eV), was equipped with a pre-treatment chamber with controlled atmosphere and temperature in which the catalyst samples could be treated under various conditions.

ICP analyses to determine the amount of metal in the solid catalyst were performed using a Perkin Elmer optima 7000 DV instrument.

2.3. Product analyses

2.3.1. HPLC

Before analyses, the catalyst was separated by centrifugation. Subsequently, 1 mL of liquid sample was neutralised using H₂SO₄ (1 M) and subsequently filtered over a syringe filter (0.45 μ m Minisart NML-cellulose acetate). 200 μ L of this sample was transferred to a HPLC vial and diluted to 500 μ L with the eluent (3 mM H₂SO₄). An injection volume of 10 μ L was used for each analysis. The samples were analysed using a Waters (HPLC instrument equipped with an Alltech IOA-1000 column maintained at 90 °C using H₂SO₄ (3 mM) in ultra-pure water as the eluent with a flow rate of 0.4 mL/min. The components were identified using an UV (210 nm) and RI detector by comparison with authentic samples. Concentrations were determined using calibration curves obtained by injecting standard solutions of known concentrations. Conversion and selectivity of various products are calculated on the basis of carbon mass. Carbon mass balance closures up to 99–100% were obtained.

2.3.2. GC–MS

To confirm the presence of lactic acid, GC–MS measurements were performed using an Interscience Trace GC equipped with a Restek GC column Rxi-5 ms (30 m \times 0.25 mm \times 0.25 μ m) connected to a Interscience Trace DSQ II XL quadrupole mass selective detector (EI, mass range 35–500 Dalton, 150 ms sample speed). Before analyses, the catalyst was removed by centrifugation and the solvent was removed in vacuo. The crude product (15 mg) was mixed thoroughly with of pyridine (0.8 mL) and of silylating agent (bis-(trimethylsilyl) trifluoroacetamide + 1% trimethylchlorosilane (0.5 mL, Regis technologies, USA)). This solution was kept at 343 K for a period of 30 min to ensure the complete silylation and subsequently injected in the GC–MS. Lactic acid was identified in the form of the bis(trimethylsilyl)lactate.

2.4. Synthesis of monometallic (Au or Pt) catalysts on nanoceria by colloidal deposition

Monometallic Au or Pt colloids were prepared by a NaBH₄ reduction method described in the literature [12,39]. HAuCl₄·3H₂O (0.042 mmol) or K₂PtCl₆ (0.042 mmol) was dissolved in 140 mL of milli-Q water containing polyvinyl alcohol (2 wt% solution, 1.9 mL) as the protecting agent. Subsequently, NaBH₄ (2.0 mL of a 0.1 M solution) was added and the pH of was adjusted to 2.5 using 0.2 M H₂SO₄. The resulting suspension was added to a suspension of nanoceria in water (2 g in 20 mL milli-Q water, sonicated for 30 min) under vigorous stirring for 3.5 h using a mechanical stirrer. The support intake was such to obtain a final metal loading of 0.4 (Au) or 0.5 (Pt) wt% in the case of monometallic *n*CeO₂ catalysts and a final total metal loading of 0.7 wt% in the case of the bimetallic (Au–Pt) *n*CeO₂ catalyst. The catalyst was separated by centrifugation and washed thoroughly with deionised water. Finally, the catalyst was dried under vacuum (0.5–2 mBar) at 323 K in the presence of a desiccant (Sicapent) for 18 h. The catalysts are designated as Au/*n*CeO₂ and Pt/*n*CeO₂ for Au on nanocrystalline ceria and Pt on nanocrystalline ceria, respectively.

Au on carbon (Au/C, 0.8 wt% Au), Au on titania (Au/TiO₂, 1 wt% Au) and Au on bulk ceria (Au/CeO₂, 0.55 wt%) were prepared by immobilising a gold colloid (prepared by the method described above) on carbon, titania and bulk ceria respectively.

2.5. Synthesis of bimetallic Au–Pt on nanoceria

Au/nanoceria (2 g) was suspended in 240 mL milli-Q water containing K₂PtCl₆ (0.0130 g) and a PVA solution (0.44 mL 2 wt%). Hydrogen gas (9.86 vol% in nitrogen) was bubbled through this slurry at a flow rate of 150 mL/min at atmospheric pressure and at room temperature for 6 h. The slurry was stirred overnight (16 h). The catalyst was isolated by centrifugation and subsequently washed with deionised water and finally dried at 323 K under vacuum (0.5–2 mBar) in the presence of desiccant (Sicapent) for 18 h. This catalyst is designated as Au–Pt/*n*CeO₂.

2.6. Catalytic experiments

Catalytic experiments were performed in 75 mL Hastelloy C-276 autoclaves (Parr Series 5000 Multiple Reactor System). The autoclave was charged with a glycerol solution (3.4 mmol) in deionised water (20 mL) followed, when appropriate, with the predetermined amount of NaOH. Subsequently, the catalyst was added (glycerol to metal ratio of 680 mol/mol) and the autoclave was closed, flushed with oxygen and finally pressurised with oxygen. The reactor contents were heated to the desired temperature under stirring with a magnetic stirring bar (600 rpm). A heating time of 10 min was required to reach the reaction temperature of 373 K (the heating time was not considered for TOF calculations). A typical reaction time was 30 min. After the specified reaction time the reactor was cooled immediately to room temperature using an ice water bath, depressurised and samples were taken for HPLC analyses.

3. Results and discussion

3.1. Catalyst synthesis and characterisation

Monometallic and bimetallic catalysts were prepared by a colloidal deposition method. Relevant properties of the catalysts are given in Table 1.

The catalysts were characterised using bright-field transmission electron microscopy (BF-TEM), scanning transmission electron microscopy (STEM), high angle annular dark field (HAADF) imaging and energy dispersive X-ray spectroscopy (XEDS). Representative

Table 1

Relevant properties of the monometallic and bimetallic Au and Pt on various supports.

Entry	Catalyst	Metal loading (wt%) ^a	Mean metal particle size (nm) ^b
1	<i>n</i> CeO ₂	–	–
2	Au/ <i>n</i> CeO ₂	0.4	3.7
3	Pt/ <i>n</i> CeO ₂	0.5	3.7
4	Au–Pt/ <i>n</i> CeO ₂	0.4 (Au), 0.3 (Pt)	3.9
5	Au/CeO ₂	0.55	4.2
6	Au/TiO ₂	1.0	4.0
7	Au/C	0.8	4.4

^a Determined by ICP-OES.

^b Determined using STEM-HAADF.

STEM and XEDS spectra for the monometallic catalysts are given in Figs. 1 (Au/*n*CeO₂) and 2 (Pt/*n*CeO₂), and Fig. 3 for the bimetallic catalyst (Au–Pt/*n*CeO₂). The average metal particle sizes for the nano ceria supported catalysts are small and all between 3.7 and 3.9 nm.

A number of particles of the bimetallic (Au–Pt/*n*CeO₂) catalyst were analysed using XEDS. Local composition of individual metal particles was obtained when the electron beam was converged to nanometer size. It showed the existence of both the metals in a single phase (Fig. 3B) which is indicative of a close interaction. This interaction was further studied by quantifying the lattice spacing using aberration-corrected atomic-resolution STEM images of the Au–Pt/*n*CeO₂ catalyst (Fig. 4c). When the (1 1 1) planes were well-resolved, the lattice spacing was found to be 0.229 nm, a value between the characteristic Au (1 1 1) and Pt (1 1 1) planes [34,40]. This proves that an Au–Pt alloy has been formed; these results are consistent with previous studies by Wang et al. [23] and Dimitratos et al. [41] on Au/Pd and later by Shen et al. [34] for Au–Pt based on lattice spacing calculations.

X-ray photoelectron spectroscopy (XPS) was used to study the chemical composition and the oxidation state of the elements at the catalyst surface. The XPS spectrum of the monometallic Au/*n*CeO₂ shows three doublets for the Au 4f core level corresponding to Au³⁺, Au⁺, and Au⁰ (Figure 2 in supporting information); the major contribution was Au⁰ (85%). The bimetallic Au–Pt/*n*CeO₂ catalyst showed the presence of Au and Pt in both the cationic as well as in the metallic state (Fig. 3D). The occurrence of cationic gold species confirms the interaction between *n*CeO₂ and Au nanoparticles, which is expected to lead to Ce³⁺ and oxygen deficient sites in the ceria. The XPS spectrum of the ceria matrix also clearly shows the Ce 3d core level having Ce³⁺ in the Au/*n*CeO₂ and Au–Pt/*n*CeO₂ catalysts (Fig. 5). In the bimetallic catalyst, the major contribution for the metal species are Au⁰ (48%) and Pt⁰ (24%), both in close interaction as derived from the EDS analysis.

3.2. Catalyst screening experiments

The one pot conversion of glycerol to lactic acid was studied in a batch reactor set-up. The reactions were typically carried out in water at a temperature of 373 K and an oxygen pressure of 5 bar using a 30 min batch time in the presence of a base (NaOH to glycerol mol ratio of 4). The glycerol to metal intake was set at 680 mol/mol. The reactions were performed using monometallic Au and Pt as well as bimetallic Au–Pt on a nanocrystalline CeO₂ support (*n*CeO₂). For the monometallic Au based catalysts, catalyst performance was compared with Au supported catalyst on conventional supports (ceria, titania and activated carbon). The results for the various experiments are summarised in Table 2. Product analyses was performed using HPLC, the presence of lactic acid was also confirmed by GC–MS after derivatisation with bis-(trimethylsilyl) trifluoroacetamide/trimethylchlorosilane.

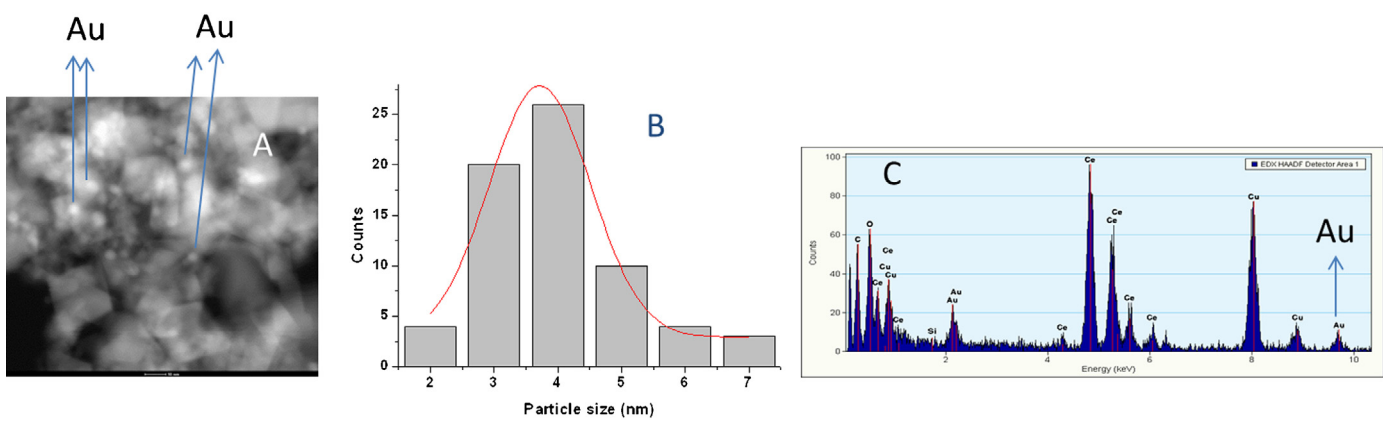


Fig. 1. STEM image of (A) Au/nCeO₂ (Scale is 10 nm) (B) particle size distribution (C) representative XEDS spectrum for an individual Au particle.

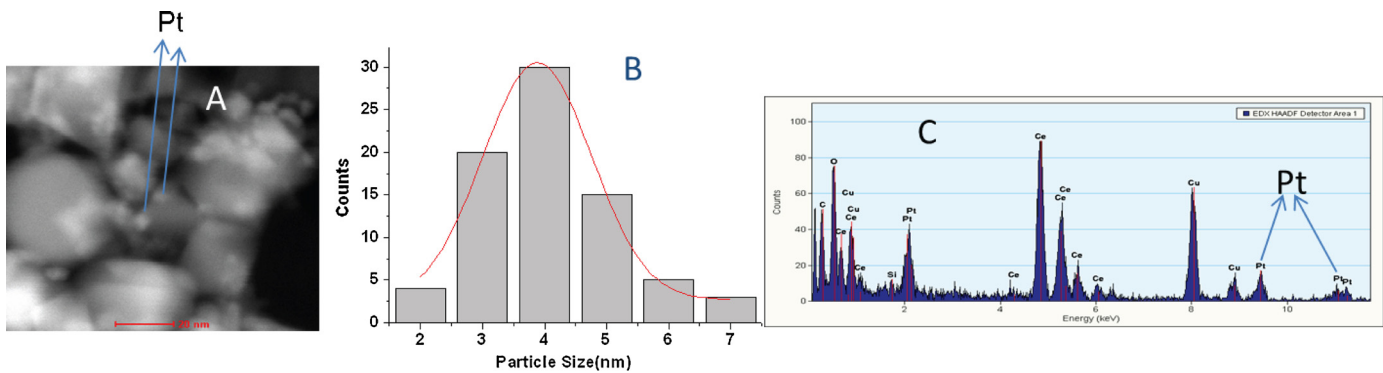


Fig. 2. STEM image of (A) Pt/nCeO₂ (Scale is 20 nm) (B) particle size distribution (C) representative XEDS spectrum for an individual Pt particle.

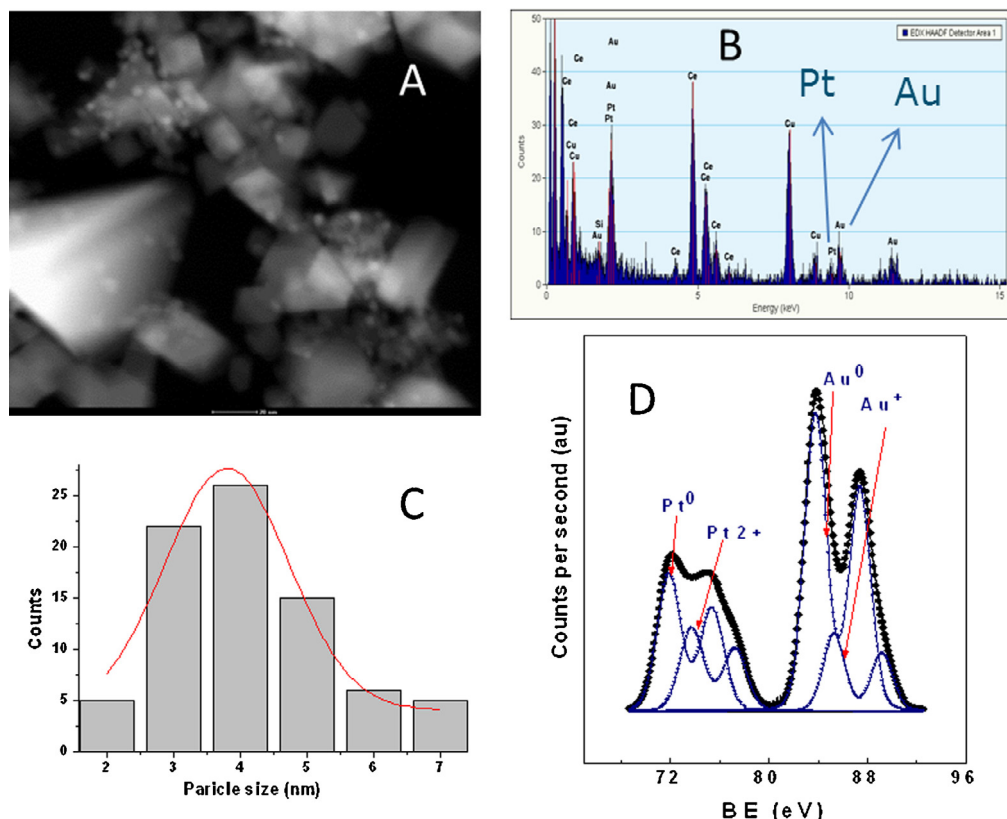


Fig. 3. (A) STEM-HAADF image for Au–Pt/nCeO₂ (scale is 20 nm) (B) representative XEDS spectrum taken for an individual single Au–Pt particle on nCeO₂ (C) particle size distribution of Au–Pt/nCeO₂ (D) XPS spectrum of Au–Pt/nCeO₂ catalyst.

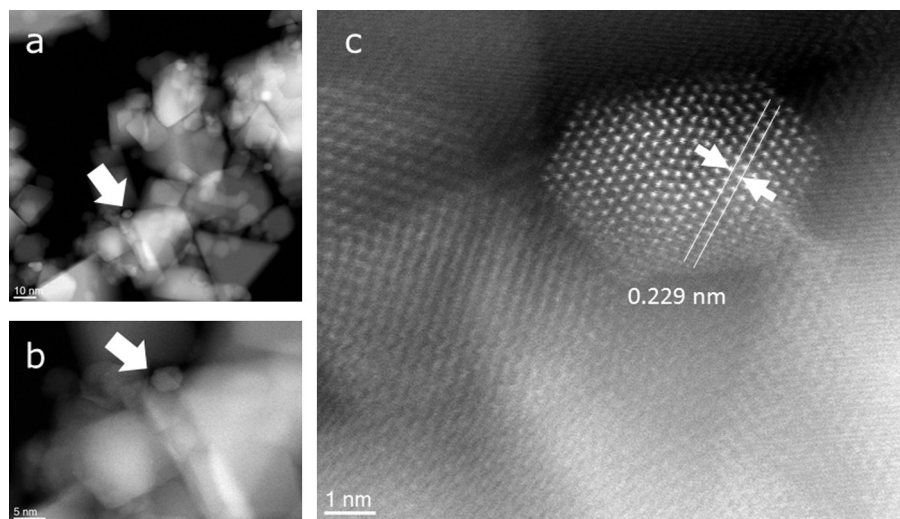


Fig. 4. High-resolution STEM pictures at different magnifications showing the nanoparticulated ceria and Au–Pt particles (a and b). The arrow indicates a bimetallic cluster that was visualised at atomic-resolution (c), indicating the lattice spacing of the (1 1 1) plane.

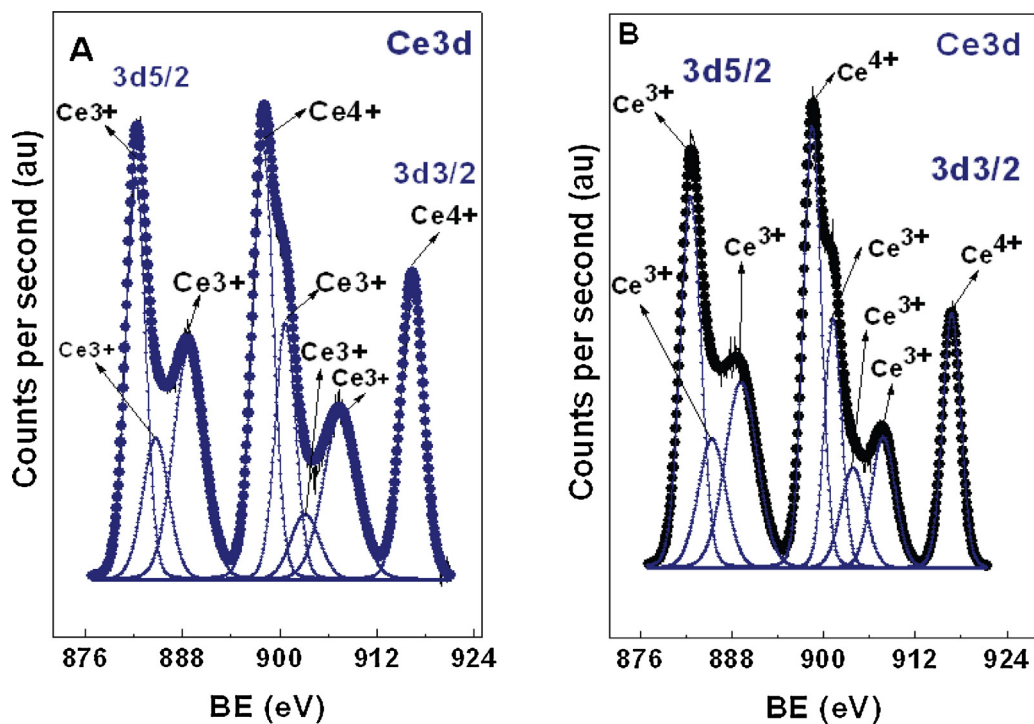


Fig. 5. XPS spectra showing the Ce 3d core level of Au/nCeO₂ (A) and Au–Pt/nCeO₂ (B).

Glycerol conversion is below 5% in the absence of a catalyst ([Table 2](#), entry 1), indicating that a hydrothermal reaction by the action of a base is not occurring to a large extent at the prevailing reaction conditions. The products, though present in minor amounts, are oxidation products like glyceric-, glycolic- and formic acid.

Initial experiments with the monometallic Au and Pt catalysts on $n\text{CeO}_2$ (Table 2, entries 2 and 3) resulted in about 80% glycerol conversion, corresponding with a catalyst TOF of about $1100 \text{ mol}/(\text{mol h}^{-1})$. The selectivity for lactic acid was 60% for Au and 68% for Pt, main by-products were glyceric acid (13–18 mol%), glycolic acid (6–7 mol%), oxalic acid (4–5 mol%) and formic acid (5–6 mol%), see Eq. (2). The formation of the latter three products is indicative for the occurrence of undesired C–C splitting reactions.

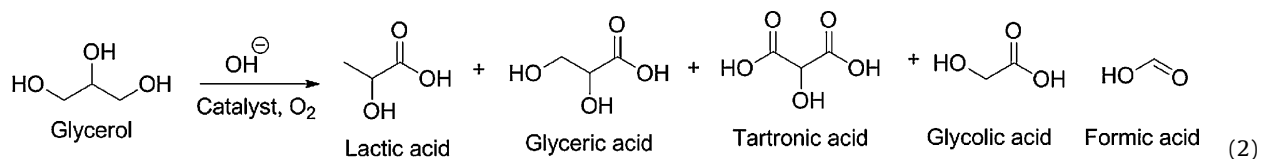


Table 2Conversion of glycerol to lactic acid using supported monometallic (Au and Pt) and bimetallic Au–Pt catalysts.^a

Entry	Catalyst	Conv. (%)	Selectivity (%)						TOF ^c (h ⁻¹)
			Lactic acid	Glyceric acid	Glycolic acid	Oxalic acid	Formic acid	Tartronic acid	
1	None	4	<1	25	50	—	24	—	—
2	Au/nCeO ₂	76	60	18	6	5	6	2	4
3	Pt/nCeO ₂	82	68	13	7	4	5	1	1120
4	Au/CeO ₂	60	52	23	8	8	6	1	820
5	Au/TiO ₂	71	45	30	2	5	2	12	970
6	Au/C ^d	83	27	50	5	<1	3	12	1130
7	Au/C	93	24	21	11	4	4	32	5
8	nCeO ₂	25	16	49	13	7	10	3	2
9	nCeO ₂ ^b	10	16	57	11	8	7	<1	—
10	Au–Pt/nCeO ₂ ^d	86	79	14	3	1	1	1	1170
11	Au–Pt/nCeO ₂	99	80	10	4	2	2	<1	1350
12	Au/nCeO ₂ + Pt/nCeO ₂ ^d	77	66	17	7	3	4	2	1040
13	Au/nCeO ₂ + Pt/nCeO ₂	90	65	15	7	5	5	2	1220

^a Reaction conditions: glycerol (0.17 M). NaOH/glycerol = 4 mol/mol, glycerol/total metal intake = 680 mol/mol, 373 K, P (O₂) = 5 bar, 30 min.^b Experiment with recycled material.^c TOF in mmol of glycerol converted per total mmol of metal per h.^d Reaction time 20 min.

The catalytic activity of the monometallic Au/nCeO₂ was compared to Au on regular (non-nanoparticulated) CeO₂ (Au/CeO₂). The mean metal particle sizes on both supports are essentially similar (3.9 vs 4.2 nm, see Table 1 for details). Catalyst performance for the nCeO₂ support was considerably better (c.f. entry 2 and 4 in Table 2) indicating that the nanoceria supports (5–25 nm particle sizes by HR-TEM, Figure 3, supporting information) is a better choice than the regular, larger sized ceria support (>50 nm by HR-STEM, Figure 4, supporting information).

Other catalyst supports (activated carbon, TiO₂) were also tested for the monometallic Au catalysts (Table 2, entries 5–7). Glycerol conversions for Au on TiO₂ are slightly lower than for the nCeO₂ support (71% vs. 76%). The selectivity to lactic acid is also reduced considerably when using TiO₂, mainly due to the formation of larger amounts of glyceric acid (up to 30 mol%). Glycerol oxidations using Au/TiO₂ have been reported in the literature. For instance, at 50 °C in basic aqueous media, glyceric acid is reported to be the main product [14] (69% selectivity at 90% glycerol conversion) and lactic acid formation is not mentioned. In contrast, Shen et al. reported that lactic acid is the main product (74% at 30% glycerol conversion) for the Au/TiO₂ catalysed conversion of glycerol in water in the presence of a base at 90 °C. Apparently, our data are consistent with the data published by Shen [34]. The use of a carbon support for Au resulted in high glycerol conversions (93%), though the main product in this case was tartronic acid (32 mol%) and lactic acid was formed in only 24% yield. Thus, remarkable support effects are observed on product selectivity and the nCeO₂ support gives the best catalyst performance for monometallic Au catalysts when lactic acid is the product of choice.

The presence of Au or Pt is essential for good catalytic performance and the use of the nano ceria support alone gave much lower glycerol conversions (25 mol%) and mainly glyceric acid as the product (49 mol%) (Table 2, entry 8). This confirms that ceria contains stoichiometric oxidation sites for alcohols, involving the Ce⁴⁺/Ce³⁺ redox couple. When subjected to a subsequent run, the activity was considerably reduced (10% conversion) (Table 2, entry 9), indicating a depletion of catalytically active cerium sites. This is in line with literature that the regeneration of catalytic sites in ceria is not occurring in the absence of metal species [36].

The use of the bimetallic Au–Pt/nCeO₂ catalyst gave a considerable improvement compared to the individual mono-metallic catalysts, a clear indication for synergic effects. The selectivity towards lactic acid increased up to a very promising 80% at near quantitative glycerol conversion (Table 2, entry 11). The synergic effect was further proven by comparing catalyst performance of the

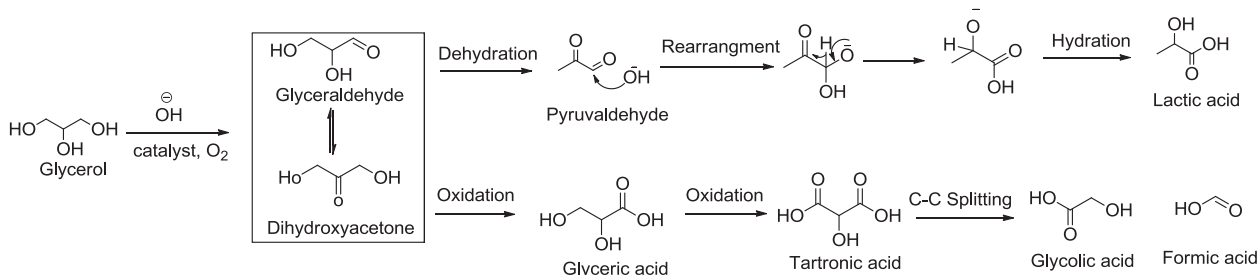
bimetallic catalyst with a physical mixture of the two monometallic ones (Table 2, entry 12). The physical mixture gave a lower glycerol conversion and a substantial lower selectivity towards lactic acid (65 vs 80 mol%) than the Au–Pt/nCeO₂ catalyst indicating a synergistic effect due to the co-existence of Au⁰ and Pt⁰ mixed clusters as evidenced by the XEDS, XPS and STEM.

3.3. Reaction pathways

A reaction network consistent with the observed product distribution and literature data is given in Scheme 1.

The network involves the initial oxidative dehydrogenation of glycerol to glyceraldehyde. In basic conditions, glyceraldehyde is in equilibrium with dihydroxyacetone [42,43]. It is well known that trioses like glyceraldehyde and dihydroxyacetone undergo rearrangement into lactic acid under alkaline conditions. As early as 1930 Shaffer and Friedmann proposed this conversion to be a base catalysed dehydration–rearrangement–dehydration, involving pyruvaldehyde (methylglyoxal) as an intermediate [44]. Kishida et al. proposed glyceraldehyde as the intermediate in the hydrothermal conversion of glycerol into lactic acid. Recently, homogeneous metal salts have also been reported to catalyse this transformation [45,46]. A parallel undesired pathway involves the catalytic oxidation of glyceraldehyde/dihydroxyacetone to glyceric acid and subsequently to further oxidation and C–C splitting products like tartronic acid, glycolic acid, oxalic acid, acetic acid and formic acid. An optimal catalyst for the conversion of glycerol into lactic acid therefore should have a strong oxidative dehydrogenation capacity under mild conditions and at the same time being a highly inefficient oxidation catalyst for the conversion of glyceraldehyde into glyceric acid and subsequent oxidation products.

The presence of a base leads has a positive effect on glycerol conversion levels (Table 3). The base is expected to deprotonate glycerol, which is known to have a positive effect on catalytic performance in metal catalysed oxidation reactions [6]. The addition of a base also enhances the selectivity to lactic acid at the expense of glyceric acid. This is in line with the proposed reaction network, where lactic acid formation from glyceraldehyde is catalysed by a base whereas the subsequent oxidation of glyceraldehyde is a metal catalysed oxidation reaction (Scheme 1). Of interest is also the presence of glyceraldehyde and pyruvaldehyde in the reaction mixtures when the reaction was performed in the absence of a base. This is a strong indication that both compounds are indeed reactive intermediates in the conversion of glycerol to lactic acid.



Scheme 1. Proposed reaction pathway for the conversion of glycerol to lactic acid and byproducts.

3.4. Effect of process conditions on catalyst performance

The effect of oxygen pressure on product selectivity was determined and the results are given in Table 4. Reactions performed in oxygen free conditions gave only 10% glycerol conversion after 3 h, yet with a 99% selectivity towards lactic acid. It is well possible that the initial oxidation of glycerol to glyceraldehyde, the initial step in the catalytic process, is catalysed by the nano-*CeO₂* support. For the stoichiometric oxidative dehydrogenation of glycerol to glyceraldehyde with CeO₂ (ceria), two moles of CeO₂ are required for one mole of glycerol. For a typical reaction, the intake of glycerol is 0.31 g (3.37 mmol) and 0.2 g (1.16 mmol) of ceria. As such, a maximum conversion of 17 mol% of glycerol is possible. In addition, reactivation of the Ce₂O₃ with molecular oxygen may occur simultaneously, leading to higher attainable glycerol conversions. The actual conversion is 10 mol%, well below the maximum levels, probably due to kinetic limitations. The occurrence of alcohol dehydrogenation instead of an oxidative dehydrogenation is possible, though thermodynamically far less favoured. The direct dehydrogenation reaction of glycerol is endothermic and typically requires high temperatures to obtain high equilibrium conversions.

An increase in oxygen pressure from 0 to 5 bar resulted in enhanced glycerol conversion rates and quantitative glycerol conversion is possible within 30 min at 5 bar and 1 h at 3 bar. Surprisingly, the lactic acid selectivity is within a narrow range (74–80 mol%) when oxygen is present. The lactic acid selectivity is determined by the relative rates of the two parallel reactions of glyceraldehyde to (i) lactic acid and (ii) glyceric acid (Scheme 1). When considering the proposed reaction network, the rate of the undesired pathway from glyceraldehyde to glyceric acid is expected to be enhanced by higher oxygen pressures, leading to higher selectivities to glyceric acid and thus a reduced lactic acid selectivity at higher oxygen pressures. This is not observed experimentally. A possible explanation is that the oxidation reaction of glyceraldehyde to glyceric acid is zero order in oxygen pressure, however, further detailed kinetic studies will be required to support this explanation. Recently, Zope et al. [6] reported on the mechanism of ethanol and glycerol oxidation to acids over various supported gold and platinum catalysts. Labelling experiments with ¹⁸O₂ and H₂ ¹⁸O demonstrate that oxygen atoms originating from hydroxide ions instead of molecular oxygen are incorporated into the alcohol during the oxidation reaction. Molecular oxygen does not participate in the catalytic cycle by dissociation to atomic

oxygen but by regenerating hydroxide ions formed via the catalytic decomposition of a peroxide intermediate. Our results are in line with these findings.

The selectivity for lactic acid formation is a function of the relative rates of the base catalysed reaction pathway to lactic acid and the oxidation pathway to glyceric acid (Scheme 1) and as such the temperature is expected to affect the selectivity of the reaction. This was also demonstrated experimentally by performing three experiments at standard conditions (30 min reaction time) with the bimetallic Au–Pt on nano-*CeO₂* catalyst at different temperatures (333, 353, 373 K), see Table 5 for details. As expected, the glycerol conversion after 30 min increased at higher temperatures, from 56% at 333 K to quantitative conversion at 373 K. The lactic acid selectivity is improved at higher temperatures, viz. 47% at 333 K and 80% at 373 K. These data imply that the reaction rate of the glyceraldehyde–lactic acid pathway has a stronger temperature dependence than the glyceraldehyde–glyceric acid pathway.

The batch experiments were performed at elevated temperature (373 K) and heating up takes about 10 min. During this non-isothermal trajectory, catalytic reactions are expected to occur. To gain insights in the extent of these reactions, a standard experiment was performed with the Au–Pt on nanoceria catalyst for which the reaction was quenched directly after reaching reaction temperature (373 K, 10 min). A 14% glycerol conversion was obtained giving mainly lactic acid (70%) and glyceric acid (21.5%). Thus, conversion, though limited, already occurs during the heating phase.

3.5. Reactivity of intermediates

The proposed reaction intermediates (glyceraldehyde, pyruvaldehyde) were only detected in considerable amounts in the product mixtures when the reactions were performed in the absence of a base (Table 3). To further assess the possible involvement of the two components in the proposed reaction sequence (Scheme 1), experiments with either glyceraldehyde or pyruvaldehyde were performed at standard conditions (373 K, NaOH (4 mol/mol substrate)) but in the absence of a catalyst and oxygen. For glyceraldehyde, full conversion of glyceraldehyde after 0.5 h and a lactic acid selectivity up to 65–70% was observed. By products such as glycolic acid (4%), formic acid (4%) were also observed along with some unidentified products. Thus, the formation of lactic acid from glyceraldehyde indeed involves a base catalysed pathway without the necessity of an oxidation

Table 3

Effect of amount of base on catalyst performance for the bimetallic Au–Pt/nCeO₂ catalyst.^a

Entry	NaOH/glycerol (mol/mol)	Conv. (%)	Selectivity (%)								
			Glyceraldehyde	Lactic acid	Glyceric acid	Glycolic acid	Oxalic acid	Formic acid	Tartronic acid	Acetic acid	Pyruvaldehyde
1	0	25	55	19	<1	—	—	—	—	—	4
2	2	60	2.0	65	15	7	3.5	3.5	1	1.5	<1
3	4	99	<1	80	10.5	4	2	2	<1	1	<1

^a 0.17 M glycerol; glycerol to metal ratio of 680 mol/mol, 373 K, P(O₂) = 5 bar, 30 min.

Table 4

Effect of oxygen pressure on catalyst performance for the bimetallic Au–Pt/nCeO₂ catalyst.^a

Entry	P(O ₂)	Time (h)	Conv. (%)	Selectivity (%)				
				Lactic acid	Glyceric acid	Glycolic acid	Oxalic acid	Formic acid
1	0	3.0	10	99	<1	0	0	0
2	1	1.0	55	77	12	6	3	2
3	3	0.5	53	76	12	5	2	4
4	3	1.0	99	74	13	5	4	3
5	5	0.5	99	80	11	4	2	2

^a Reaction conditions: 0.17 M glycerol; NaOH/glycerol = 4 mol/mol, glycerol/metal = 680 mol/mol, 373 K.

Table 5

Effect of temperature on catalyst performance for the bimetallic Au–Pt/nCeO₂ catalyst.^a

Temperature (K)	Conv. (%)	Selectivity (%)					
		Lactic acid	Glyceric acid	Glycolic acid	Oxalic acid	Formic acid	Tartronic acid
333	56	47	33	6	3	7	3
353	98	58	24	5	2.5	5	4
373	99	80	10.5	4	2.0	2	0.5

^a Reaction conditions: 0.17 M NaOH/glycerol = 4 mol/mol, glycerol/metal = 680 mol/mol, 30 min.

Table 6

Catalytic experiments with glyceric acid and lactic acid using the bimetallic Au–Pt/nCeO₂ catalyst.^a

Entry	Substrate	Time (h)	Conv. (%)	Selectivity					
				Lactic acid	Glyceric acid	Glycolic acid	Oxalic acid	Formic acid	Tartronic acid
1	Glyceric acid	0.5	38	0	0	6	10	3.5	76
2	Lactic acid	0.5	0	–	–	–	–	–	–
3	Lactic acid	3.5	5.0	0	1	0	15	0	26
									52

^a Reaction conditions: 0.17 M substrate, NaOH/substrate = 4 mol/mol, 373 K, P(O₂) = 5 bar, substrate/metal = 680 mol/mol.

catalyst. Experiments starting with pure pyruvaldehyde, in the presence of NaOH (NaOH to pyruvaldehyde mol ratio of 4) resulted in quantitative conversion of pyruvaldehyde within 5–8 min at room temperature to lactic acid in quantitative yields.

The formation of over oxidation and C–C scission products like tartronic acid, glycolic acid, acetic acid and formic acid were observed for all catalytic experiments. To gain insights whether these are formed in the glyceric acid or lactic acid pathway (**Scheme 1**), catalytic experiments were performed with glyceric acid and lactic acid as the starting materials. The results are depicted in **Table 6**.

Lactic acid conversion was not observed after 30 min reaction, a typical reaction time for a catalytic experiment with glycerol. Extended times (3.5 h) resulted in 5% lactic acid conversion to acetic acid, oxalic acid and tartronic acid. Thus, lactic acid is prone to further oxidation reactions, though the conversion is negligible at standard reaction time (30 min) for the glycerol oxidation reaction due to low reaction rates. Experiments with glyceric acid at standard conditions for glycerol experiments resulted in 38% conversion after 30 min, the main products being tartronic acid as well as scission products such as glycolic acid, oxalic acid, acetic acid and formic acid. Apparently, glyceric acid is not stable at reaction conditions and is the major source of other (smaller) organic acids.

3.6. Optimisation of catalyst performance

Lactic acid is a typical bulk chemical product with high production volumes. Novel routes should comply with the green chemistry and technology principles and as such, catalyst stability and reduction of solvent usage are of pivotal importance. The catalyst stability for the bimetallic Au–Pt/nCeO₂ catalyst was tested by performing a number of recycle runs in the batch set-up. After each reaction, the catalyst was recovered by centrifugation, washed with an excess of water and dried (50 °C in vacuum for 16 h in the presence of sapicent). The results are shown in **Fig. 6**. Catalyst stability is good

and loss of activity and selectivity was not observed after 4 recycle runs. In line with these findings is the absence of Au and Pt in the liquid phase after reaction (ICP-OES), indicating that catalyst leaching does not occur to a significant extent. The cumulative TON was 3400 mol/(mol metal intake).

To reduce solvent usage, a number of experiments was performed at higher glycerol concentrations (**Table 7**), while all other reaction conditions (including metal intake) were at standard values.

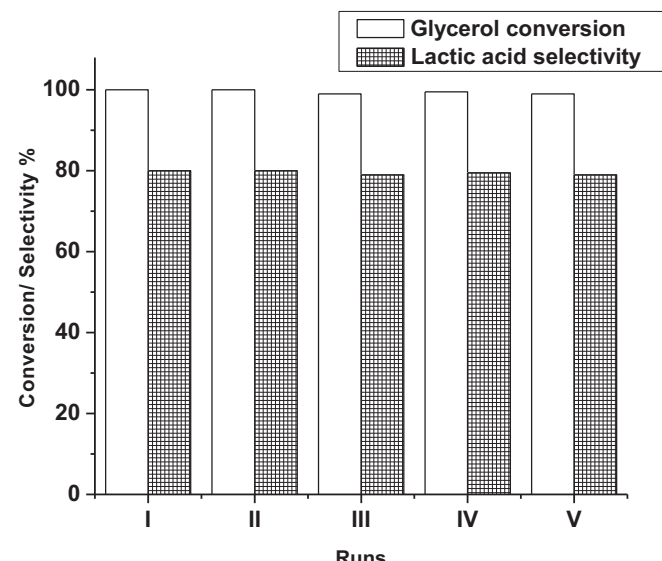


Fig. 6. Recycle experiments for Au–Pt nCeO₂ (conditions for each experiment: 0.17 M glycerol, NaOH to glycerol mol ratio of 4, glycerol to metal mol ratio of 680, 100 °C, P(O₂) = 5 bar, 30 min).

Table 7Effect of glycerol concentration on performance of the Au–Pt/nCeO₂ catalyst.^a

Entry	Glycerol con. (M)	Time (h)	Conv. (%)	Selectivity (%)							TOF (h ⁻¹)
				Lactic acid	Glyceric acid	Glycolic acid	Oxalic acid	Formic acid	Tartronic acid	Acetic acid	
1	0.17	0.5	99	80	10.5	4	2	2	<1	1	>1350
		0.5	56	79	9	5	2	3	1	1	1520
2	0.34	1.0	99	77	6	6	3	4	1.5	1.5	>1320
		0.5	24.5	81	4	6	1	4	1.5	2.5	1330
3	0.6	2.0	75	77	9	5	2	4.5	1.5	1	1020

^a Reaction conditions: Deionised water (20 mL), NaOH/glycerol = 4 mol/mol, 373 K, P(O₂) = 5 bar, glycerol/metal ratio for entry 1 = 680 mol/mol, entry 2 = 1360 mol/mol, entry 3 = 2720 mol/mol. TOF in mmol of glycerol converted/total mmol of metal/h.

Based on the data, it can be concluded that the Au–Pt/nCeO₂ catalyst remains active even at high concentration of glycerol without a significant drop in the selectivity towards lactic acid.

4. Conclusions

Monometallic Au and Pt based catalyst on a commercially available nanocrystalline CeO₂ support are efficient catalysts for the one pot oxidative conversion of glycerol to lactic acid. For Au, the nano-ceria support shows better performance than non-nanoparticulated CeO₂, activated carbon and TiO₂. Further improvements are possible by the application of bimetallic Au–Pt/nCeO₂ catalysts. Lactic acid yields of up to 80% were obtained at a TOF of 1170 mol/(mol h⁻¹) for a 20 min batchtime; main byproducts are glyceric acid and subsequent oxidation products (such as tartronic acid, glycolic acid, formic acid and acetic acid). The Au–Pt/nCeO₂ catalyst was shown to be reusable without loss in activity and lactic acid selectivity for five successive batch runs. A reaction pathway is proposed and the involvement of intermediates is supported by additional experiments with pure intermediates.

The synthetic methodology largely complies with the twelve principles of green chemistry. It uses a renewable feed for the synthesis of an existing bulk chemical (lactic acid) with high application potential, uses a catalytic route with a catalyst that has shown to be recyclable at least five times, suggesting reasonable/good stability, is carbon atom efficient, uses an environmentally benign oxidant (oxygen), is carried out in a single step in good yields, and uses an environmentally benign solvent (water). The main point of concern is the need of a soluble base (NaOH) to give improved catalyst activity, leading to the formation of the lactate after reaction, that needs to be neutralised to give lactic acid and as such produces significant amounts of salt. Therefore, the development for catalytic methodology without the need of a base is high on the research agenda.

Acknowledgements

This research was performed in the framework of the NWO-ASPECT programme (The Netherlands). Stefan Hollak and Rob Gosselink (University of Utrecht) are acknowledged for electron microscopy measurements, Andries Jekel for ICP-OES analysis and Prof. J.L.G. Fierro (Instituto de Catalisis y Petroleoquímica, CSIC, Madrid) for XPS measurements. The Laboratorio de Microscopias Avanzadas (LMA) in the Institute of Nanoscience of Aragon (INA), University of Zaragoza (Dr. Alvaro Mayoral) is acknowledged for electron microscopy support.

Appendix A. Supplementary data

Supplementary data associated with this article can be found, in the online version, at <http://dx.doi.org/10.1016/j.apcatb.2013.07.068>.

References

- [1] C.-H. Zhou, J.N. Beltramini, Y.-X. Fan, G.Q. Lu, *Chem. Soc. Rev.* 37 (2008) 527–549.
- [2] A. Corma, S. Iborra, A. Velty, *Chem. Rev.* 107 (2007) 2411–2502.
- [3] B. Katryniok, H. Kimura, E. Skrzynska, J.-S. Girardon, P. Fongarland, M. Capron, R. Ducoulombier, N. Mimura, S. Paul, F. Dumeignil, *Green Chem.* 13 (2011) 1960–1979.
- [4] M. Haruta, *Nature* 437 (2005) 1098–1099.
- [5] G.J. Hutchings, *Chem. Commun.* (2008) 1148–1164.
- [6] B.N. Zope, D.D. Hibbitts, M. Neurock, R.J. Davis, *Science* 330 (2010) 74–78.
- [7] A.S.K. Hashmi, G.J. Hutchings, *Angew. Chem. Int. Ed.* 45 (2006) 7896–7936.
- [8] C.W. Corti, R.J. Holliday, D.T. Thompson, *Appl. Catal. A: Gen.* 291 (2005) 253–261.
- [9] G.J. Hutchings, M. Haruta, *Appl. Catal. A: Gen.* 291 (2005) 2–5.
- [10] C. Della Pina, E. Faletta, L. Prati, M. Rossi, *Chem. Soc. Rev.* 37 (2008) 2077–2095.
- [11] S. Carreton, P. McMorn, P. Johnston, K. Griffin, G.J. Hutchings, *Chem. Commun.* (2002) 696–697.
- [12] F. Porta, L. Prati, *J. Catal.* 224 (2004) 397–403.
- [13] S. Demirel-Gülen, M. Lucas, P. Claus, *Catal. Today* 102–103 (2005) 166–172.
- [14] N. Dimitratos, A. Villa, C.L. Bianchi, L. Prati, M. Makkee, *Appl. Catal. A: Gen.* 311 (2006) 185–192.
- [15] S. Carreton, P. Concepción, A. Corma, J.M. López Nieto, V.F. Puntes, *Angew. Chem. Int. Ed.* 43 (2004) 2538–2540.
- [16] M. Comotti, W.-C. Li, B. Spliethoff, F. Schüth, *J. Am. Chem. Soc.* 128 (2005) 917–924.
- [17] C.L. Bianchi, P. Canton, N. Dimitratos, F. Porta, L. Prati, *Catal. Today* 102–103 (2005) 203–212.
- [18] N. Dimitratos, F. Porta, L. Prati, *Appl. Catal. A: Gen.* 291 (2005) 210–214.
- [19] S. Demirel, K. Lehnert, M. Lucas, P. Claus, *Appl. Catal. B: Environ.* 70 (2007) 637–643.
- [20] W.C. Ketchie, M. Murayama, R.J. Davis, *J. Catal.* 250 (2007) 264–273.
- [21] L. Prati, A. Villa, F. Porta, D. Wang, D. Su, *Catal. Today* 122 (2007) 386–390.
- [22] A. Villa, G.M. Veith, L. Prati, *Angew. Chem. Int. Ed.* 49 (2010) 4499–4502.
- [23] D. Wang, A. Villa, F. Porta, D. Su, L. Prati, *Chem. Commun.* (2006) 1956–1958.
- [24] Y.J. Wee, J.N. Kim, H.W. Ryu, *Food Technol. Biotechnol.* 44 (2006) 163–172.
- [25] C.S.M. Pereira, V.M.T.M. Silva, A.E. Rodrigues, *Green Chem.* 13 (2011) 2658–2671.
- [26] B. Katryniok, S. Paul, F. Dumeignil, *Green Chem.* 12 (2010) 1910–1913.
- [27] Y. Fan, C. Zhou, X. Zhu, *Catal. Rev.* 51 (2009) 293–324.
- [28] H. Kishida, F. Jin, Z. Zhou, T. Moriya, H. Enomoto, *Chem. Lett.* 34 (2005) 1560–1561.
- [29] C.A. Ramírez-Lo'pez, J.R. Ochoa-Go'mez, M. a. Fernández-Santos, O. Go'mez-Jiménez-Aberasturi, A. Alonso-Vicario, J.S. Torrecilla-Soria, *Ind. Eng. Chem. Res.* 49 (2010) 6270–6278.
- [30] Z. Shen, F. Jin, Y. Zhang, B. Wu, A. Kishita, K. Tohji, H. Kishida, *Ind. Eng. Chem. Res.* 48 (2009) 8920–8925.
- [31] E.P. Maris, W.C. Ketchie, M. Murayama, R.J. Davis, *J. Catal.* 251 (2007) 281–294.
- [32] E.P. Maris, R.J. Davis, *J. Catal.* 249 (2007) 328–337.
- [33] J. ten Dam, F. Kapteijn, K. Djanashvili, U. Hanefeld, *Catal. Commun.* 13 (2011) 1–5.
- [34] Y. Shen, S. Zhang, H. Li, Y. Ren, H. Liu, *Chem. Eur. J.* 16 (2010) 7368–7371.
- [35] F. Auneau, S. Noël, G. Aubert, M. Besson, L. Djakovitch, C. Pinel, *Catal. Commun.* 16 (2011) 144–149.
- [36] A. Abad, P. Concepción, A. Corma, H. García, *Angew. Chem. Int. Ed.* 44 (2005) 4066–4069.
- [37] J. Guzman, S. Carreton, A. Corma, *J. Am. Chem. Soc.* 127 (2005) 3286–3287.
- [38] G.L. Brett, P.J. Miedziak, N. Dimitratos, J.A. Lopez-Sánchez, N.F. Dummer, R. Tirumvalam, C.J. Kiely, D.W. Knight, S.H. Taylor, D.J. Morgan, A.F. Carley, G.J. Hutchings, *Catal. Sci. Technol.* (2011).
- [39] R.G. Discipio, *Anal. Biochem.* 236 (1996) 168–170.
- [40] S.C.Y. Tsen, P.A. Crozier, J. Liu, *Ultramicroscopy* 98 (2003) 63–72.
- [41] N. Dimitratos, A. Villa, D. Wang, F. Porta, D. Su, L. Prati, *J. Catal.* 244 (2006) 113–121.
- [42] V.A. Yaylayan, S. Harty-Majors, A.A. Ismail, *Carbohydr. Res.* 318 (1999) 20–25.
- [43] R.W. Nagorski, J.P. Richard, *J. Am. Chem. Soc.* 123 (2001) 794–802.
- [44] P.A.S.A.E. Friedemann, *J. Biol. Chem.* 86 (1930) 345–374.
- [45] C.B. Rasrendra, B.A. Fachri, I.G.B.N. Makertihartha, S. Adisasmto, H.J. Heeres, *ChemSusChem* 4 (2011) 768–777.
- [46] Y. Hayashi, Y. Sasaki, *Chem. Commun.* (2005) 2716–2718.